Clays and Clay Minerals, Vol. 56, No. 2, 175–189, 2008.

PARTITIONING OF Fe(II) IN REDUCED NONTRONITE (NAu-2) TO REACTIVE SITES: REACTIVITY IN TERMS OF Tc(VII) REDUCTION

DEB P. JAISI[1,2], HAILIANG DONG[1,*], AND JOHN P. MORTON[1]

[1] Department of Geology, Miami University, Oxford, OH 45056, USA
[2] Department of Geology and Geophysics, Yale University, PO Box 20820, New Haven, CT 06520, USA

Abstract—Clay minerals impart important chemical properties to soils, in part, by virtue of changes in the redox state of Fe in their crystal structures. Therefore, measurement of Fe(III)/Fe(II) and partitioning of Fe(II) in different reactive sites in clay minerals (during biological and chemical Fe(III) reduction) is essential to understand their role and their relative reactivity in terms of reduction and immobilization of heavy metal contaminants such as technetium. This study had three objectives: (1) to understand the degree of dissolution of nontronite (Fe-rich smectite) as a result of chemical and biological reduction of Fe(III) in the structure; (2) to quantify partitioning of chemically and biologically produced Fe(II) into different reactive sites in reduced nontronite, including aqueous Fe^{2+}, ammonium chloride-extractable Fe(II) (mainly from the ion-exchangeable sites, denoted as $Fe(II)_{NH_4Cl}$), sodium acetate-extractable Fe(II) (mainly from the surface complexation sites, denoted as $Fe(II)_{acetate}$), and structural Fe(II) (denoted as $Fe(II)_{str}$); and (3) to evaluate the reactivity of these Fe(II) species in terms of Tc(VII) reduction. Chemical and biological reduction of Fe(III) in nontronite (NAu-2) was performed, and reduced nontronite samples with different extents of Fe(III) reduction (1.2−71%) were prepared. The extent of reductive dissolution was measured as a function of the extent of Fe(III) reduction. Our results demonstrated that chemically and biologically produced Fe(II) in NAu-2 may be accommodated in the NAu-2 structure if the extent of Fe(III) reduction is small (< ~30%). When the extent of reduction was >~30%, dissolution of nontronite occurred with a corresponding decrease in crystallinity of residual nontronite. The Fe(II) produced was available for partitioning into four species: $Fe^{2+}_{(aq)}$, $Fe(II)_{acetate}$, $Fe(II)_{NH_4Cl}$, and $Fe(II)_{str}$. The increase in $Fe(II)_{acetate}$ during the early stages of Fe(III) reduction indicated that the Fe(II) released had the greatest affinity for the surface-complexation sites, but this site had a limited capacity (~60 μmol of Fe(II)/g of NAu-2). The subsequent increase in $Fe(II)_{NH_4Cl}$ indicated that the released Fe(II) partitioned into the exchangeable sites once the amount of Fe at the surface-complexation sites reached half of its maximum site capacity. The fraction of $Fe(II)_{str}$ decreased concomitantly, as a result of Fe(II) release from the NAu-2 structure, from 100% when the extent of Fe(III) reduction was <30% to nearly 65% when the extent of Fe(III) reduction reached 71%. The $Fe(II)_{acetate}$ and $Fe(II)_{str}$ exhibited greater reactivity in terms of Tc(VII) reduction than the $Fe(II)_{NH_4Cl}$. Clearly, the surface-complexed and structural Fe(II) are the desirable species when reduced clay minerals are used to reduce and immobilize soluble heavy metals in contaminated groundwater and soils. These results have important implications for understanding microbe−clay mineral interactions and heavy metal immobilization in clay-rich natural environments.

Key Words—Fe(III) Reduction, Fe(II) partitioning, *Shewanella putrefaciens* CN32, NAu-2, Tc(VII) Reduction.

INTRODUCTION

Clay minerals play an important role in environmental processes such as nutrient cycling, plant growth, contaminant migration, organic-matter maturation, and petroleum production (Stucki *et al*., 2002; Kim *et al*., 2004; Stucki, 2006). Iron is a major constituent in clays and clay minerals, and its mobility and stability in different environmental processes are, in part, controlled by the oxidation state (Stucki *et al*., 2002). The structural ferric Fe in clay minerals can be reduced either chemically or biologically (Gates *et al*., 1993; Kostka *et al*., 1996, 1999; Dong *et al*., 2003a, 2003b; Kim *et al*., 2004; Jaisi *et al*., 2005, 2007a, 2007b; O'Reilly *et al*., 2005, 2006; Stucki, 2006; Stucki and Kostka, 2006). Although these studies have consistently shown that the extent of Fe(III) reduction is a function of different parameters such as cell and clay concentration, crystal-chemical environments, the amount of Fe(III) in clay structures, solution chemistry, and growth/non-growth media, the fate of Fe(II) produced by chemical and biological reduction of Fe(III) in clay minerals is still poorly understood.

The extant literature reports starkly contrasting results on Fe(II) partitioning in reduced (either chemically or biologically) smectites. In one extreme, it is reported that all Fe(II) is accommodated in the smectite crystal structure with some structural modifications (Manceau *et al*., 2000a, 2000b), suggesting that reduction of Fe(III) to Fe(II) occurs primarily in a solid state (Lee *et al*., 2006). Consistent with this solid-state

* E-mail address of corresponding author:
dongh@muohio.edu
DOI: 10.1346/CCMN.2008.0560204

reduction mechanism, multiple studies (Fialips *et al*., 2002; Favre *et al*., 2006; Lee *et al*., 2006; Komadel *et al*., 2006; Stucki, 2006; Stucki and Kostka, 2006) have found that upon reoxidation, fully or partially reduced smectites (both by chemical and biological methods) can mostly be restored to the unaltered state. One study reported that partial dehydroxylation and redistribution of Fe, and perhaps Al, from Fe(III) reduction was not fully recoverable upon reoxidation (Fialips *et al*., 2002). In contrast to the solid-state reduction mechanism, other studies have shown partial dissolution of reactant smectite (Dong *et al*., 2003a, 2003b) and formation of biogenic minerals such as illite, siderite, and vivianite as a result of bacterial reduction of Fe(III) in smectites (Kim *et al*., 2004; Li *et al*., 2004). O'Reilly *et al*. (2005, 2006) and Furukawa and O'Reilly (2006) reported dissolution of nontronite and release of structural Fe, even before the onset of Fe(III) bioreduction. Chemically and biologically produced Fe(II) in reduced nontronite may be partially released and partitioned into four different reactive sites, *i.e.* aqueous, surface-complexation, ion-exchangeable, and structural (Hoffstetter *et al*., 2003, 2006). These species may exhibit different reactivity in terms of degradation of nitroaromatic compounds (Hoffstetter *et al*., 2003, 2006). In order to understand the relative reactivity of these various Fe(II) species in terms of heavy metal reduction and immobilization, it is important to quantify Fe(II) partitioning in reduced clay minerals such as nontronite.

^{99}Tc, a predominantly nuclear reaction product, is a significant contaminant at several US Department of Energy (DOE) sites (Riley and Zachara, 1992) because of its long half-life (2.13×10^5 y), its mobility (as $^{99}TcO_4^-$), and subsequent uptake into the food chain (Cataldo *et al*., 1989). For example, at the Hanford site in Washington State, there exist four large ^{99}Tc plumes and new ones are forming as a result of continued leakage (Fredrickson *et al*., 2004). Due to a very low partitioning coefficient (K_d) of ^{99}Tc(VII) in the Hanford soil (0−0.1 mL/g; Cantrell *et al*., 2003), pertechnetate (TcO_4^-) behaves as a conservative tracer and hence moves nearly unimpeded with groundwater. Present forecasts suggest that >1480 GBq of TcO_4^- may potentially be discharged into the Columbia River in the future (Fredrickson *et al*., 2004), and therefore it poses an immediate problem to the major watershed of the Pacific Northwest.

The redox geochemistry of ^{99}Tc is dominated by Tc(IV) and Tc(VII), two stable valence states of Tc (Bratu *et al*., 1975). The mobility of Tc(VII) is substantially decreased under reducing conditions (Albinsson *et al*., 1991) when soluble $Tc(VII)O_{4\,(aq)}^-$ is transformed to relatively insoluble $Tc(IV)O_{2(s)}$ (Lieser and Bauscher, 1988; Wildung *et al*., 2000; Hess *et al*., 2004). Previous studies have shown that Fe(II) produced from microbial reduction of natural sediments (Fredrickson *et al*., 2004) or Fe(II) associated with natural soils and sediments (Cui and Ericksen, 1996; Lloyd *et al*., 2000; Wildung *et al*., 2004; Burke *et al*., 2005) is effective in reducing Tc(VII) to Tc(IV). These results imply that Fe(II) in clay minerals may be used as an effective reductant for heterogeneous reduction of Tc(VII). However, the role of Fe(II) in clay minerals, especially in smectite, in reduction of Tc(VII) has not been investigated. As clay and clay-like minerals (smectite, illite, chlorite, biotite) are commonly present at DOE sites (Fredrickson *et al*., 2004; Qafoku *et al*., 2003; Kukkadapu *et al*., 2006), and they are potential backfill materials for nuclear-waste repositories (Giaquinta *et al*., 1997; NAGRA, 2002), understanding the interaction of clay minerals with radionuclides such as Tc is important.

Among different Fe(II) species in smectite, Fe(II) at surface-complexation and structural sites has been found to be reactive for reduction of Cr(VI) (Gan *et al*., 1996; Taylor *et al*., 2000), organic compounds (Hofstetter *et al*., 2003, 2006), and possibly for U(VI) and Tc(VII) as well (Stucki, 2006). However, the reactivity of Fe(II) species in one smectite may be grossly different from that in another due to variation of intrinsic properties such as location of the Fe, the presence or absence of other structural and interlayer cations, the degree of swelling, and the hydration of interlayer cations (Cervini-Silva, 2004; Cervini-Silva *et al*., 2006). Determining the relative partitioning of Fe(II) into various reactive sites of different smectites as a function of Fe(III) reduction is, therefore, important.

Our results show that Fe(II) partitions into four different reactive sites and their partitioning is a function of Fe(III) reduction. These Fe(II) species are found to be reactive in reducing Tc but to have different degrees of reactivity.

MATERIALS AND METHODS

Mineral, media, and reagent preparation

Clay-mineral preparation. The bulk sample of nontronite [NAu-2: $M_{0.72}^+(Fe_{3.83}Mg_{0.05})(Al_{0.45}Si_{7.55})O_{20}(OH)_4$, where *M* may be Ca, Na, or K (Keeling *et al*., 2000)] was purchased from the Source Clays Repository, of The Clay Minerals Society, located at Purdue University, Indiana. The sample was soaked thoroughly, sonicated briefly in an ultrasonic water bath, and then centrifuged in order to obtain the <0.2 μm size fraction. This size fraction was characterized by direct current plasma (DCP) emission spectroscopy, chemical extraction, Mössbauer spectroscopy for Fe(II) and Fe(III) content; and X-ray diffraction (XRD) and transmission electron microscopy (TEM) for mineralogy and morphology. Briefly, the treated NAu-2 was pure, and contained 23.4% total Fe in its structure, with almost all (99.8%) of the Fe as Fe(III) (Jaisi *et al*., 2005, 2007a, 2007b). Keeling *et al*. (2000) and Gates *et al*. (2002) reported

minor amounts (~1%) of carbonate impurities and possibly some Fe oxyhydroxides in the <0.15 μm size fraction.

To understand the role of interlayer cation composition in the electron-transfer process, the <0.2 μm size fraction of NAu-2 was converted into Na and K homoionic forms by the ion exchange process (Bukka *et al*., 1992; Baeyens and Bradburry, 1997; Bradbury and Baeyens, 2002; Hofstetter *et al*., 2003). The preparation of the homoionic forms was carried out by subjecting the size-separated NAu-2 to repetitive ion exchange (four times) with aqueous (1.0 M) chloride salt solutions containing either Na or K cation (Bukka *et al*., 1992). The total concentration of the cation in the chloride salt solution corresponded to at least five times the cation exchange capacity (CEC) of NAu-2 (639.45 (±11.20) meq/kg; Jaisi *et al*., unpublished results). Each of the repetitive exchange reactions was carried out for a period of 24 h with constant, slow stirring at room temperature. The homoionized, <0.2 μm size fraction of NAu-2 was dialyzed in deionized (DI) water for 1 week, using fresh DI water twice each day to remove any residual cations and chloride. After freeze-drying, these homoionized samples were analyzed by XRD to confirm the collapsed layer spacing (10 Å). These samples were used to assess the effect of interlayer cation composition on microbial reduction of Fe(III) in the NAu-2 structure.

Bacterial culture. *Shewanella putrefaciens* CN32 cells were routinely cultured aerobically in a tryptic soy broth (TSB) from frozen stock culture, which was kept in 40% glycerol at −80ºC. After harvesting in TSB until the mid- to late-log phase, CN32 cells were washed three times (4 min each) by centrifugation at 4000 g and re-suspended using: (1) Na-bicarbonate buffer (2 g/L of reagent grade $NaHCO_3$, and 0.1 g/L of KCl) for the experiment designed to study the Fe(II) partitioning; and (2) 30 mM of PIPES (1,4-piperazine diethanesulfonic acid) buffer for the experiments designed to understand the role of interlayer cation composition (Na and K) in the electron transfer.

Fe(III) reduction in NAu-2

Biologically mediated Fe(III) reduction. Experiments involving biological Fe(III) reduction were performed following our previously described procedure (Jaisi *et al*., 2005) in Na-bicarbonate buffer. NAu-2 and cell concentration were fixed at 5 mg/mL and ~1×10^8/mL, respectively. To understand the role of interlayer cation composition in the electron-transfer process, bioreduction experiments were performed in PIPES buffer using the homoionized, < 0.2 μm size fraction and the CN32 cells prepared in the same buffer. All experiments were performed in duplicate. To prepare different levels of Fe(III) reduction, bioreduction was stopped at pre-determined times, by means of pasteurization (at 80ºC for 3 h). The extent of bioreduction and Fe(II) partitioning was measured (see below).

Chemical Fe(III) reduction. Chemically reduced NAu-2 was prepared by adding a known amount of dithionite to a solution containing NAu-2 (final concentration of 5 mg/mL) in an anaerobic buffer (266 mM sodium citrate and 111 mM sodium bicarbonate buffer, Stucki *et al*., 1984a). The amount of dithionite required to achieve a certain extent of Fe(III) reduction was calculated based on a few preliminary experiments and the reaction stoichiometry. Each experiment was allowed to run for 5 days based on our previous experience (Jaisi *et al*., 2007b). The extent of reduction and Fe(II) partitioning was measured (see below).

X-ray diffraction

All NAu-2 samples, including the unreduced, homoionized, chemically and biologically reduced, were studied by XRD. For the homoionized NAu-2, confirming the collapsed interlayer spacing was important. For the reduced samples, identifying changes in crystallinity as a function of the extent of Fe(III) reduction was important. The oriented mounts of the samples were air-dried in either air or an anaerobic glove box (95% N_2 and 5% H_2) (Coy Laboratory Products, Grass Lake MI). The XRD patterns were collected with a Scintag X1 powder diffractometer system using CuKα radiation with a variable divergence slit and a solid-state detector. Low-background quartz XRD slides (Gem Dugout, Inc., Pittsburgh, Pennsylvania) were used for calibration.

Measurement of Fe(II) partitioning in Fe(III)-reduced NAu-2

HCl-extractable Fe(II) produced by Fe(III) reduction was measured by 0.5 N HCl extraction followed by Ferrozine assay (Stookey, 1970), and total Fe(II) by total dissolution using HF (Andrade *et al*., 2002). For clarity, and in order to comply with the convention of expressing Fe(III) reduction based on 0.5 N HCl extraction (Fredrickson *et al*., 1998; Zachara *et al*., 1998), all reported values in this communication were 0.5 N HCl extraction results, unless specifically referred to as 'total dissolution.' The extracted Fe(II) and other dissolved cations from both biologically and chemically reduced NAu-2 were measured by direct current plasma (DCP) emission spectrometry (Katoh *et al*., 1999) and inductively coupled plasma mass spectrometry (ICP-MS) methods to quantify NAu-2 dissolution and to calculate mass balance.

$Fe^{2+}_{(aq)}$ concentration was determined in the supernatant following centrifugation of the reduced NAu-2 suspensions. Ammonium chloride is effective in displacing cations from ion-exchangeable sites and it is commonly used in the determination of the CEC of clay minerals and soils (Skinner *et al*., 2001). Therefore, this extraction was presumed to be effective at extracting

Fe(II) from ion-exchangeable sites and was termed $Fe(II)_{NH_4Cl}$. Briefly, reduced NAu-2 was extracted twice with 200 mM ammonium chloride at pH 7.0 for a maximum of 1 h under absolutely anoxic conditions. The NAu-2 suspension was centrifuged and mass recorded to determine any entrained extractant. Any extractable Fe(II) remaining after this extraction was presumed to be associated with the surface complexation (amphoteric/variable surface charge) sites and could be desorbed by Na acetate ($Fe(II)_{acetate}$) (Bradbury and Baeyens, 1997; Jaisi *et al.*, unpublished results). The same sample (after the ammonium chloride extraction) was immediately extracted for 4 h with absolutely anoxic 1 M Na acetate buffered at pH 4.25.

The pH 7.0 extract was analyzed for Fe(II) and other ion exchangeable cations to define the total adsorbed cation charge. Similarly, the pH 4.25 extract was analyzed for Fe(II) and NH_4^+ to determine the total adsorbed cation charge and to calculate mass balance with the pH 7.0 extract. If a significant difference was found in mass balance, the pH 4.25 Na-acetate extraction was followed with lanthanum nitrate extraction to desorb exchangeable Al. The amount of Fe(II) in the pH 7.0 extract was termed $Fe(II)_{NH_4Cl}$, while that in the pH 4.25 extract was termed $Fe(II)_{acetate}$. The amount of Fe(II) remaining in the reduced NAu-2 samples after these extractions was termed structural Fe(II) (denoted as $Fe(II)_{str}$). Structural Fe(II) was extracted by reacting the residual NAu-2 with 0.5 N HCl. All these experiments were performed under absolutely anoxic conditions. The presence of contaminant oxygen was checked using a CHEMets® colorimetric analysis kit R-7540 (2.5 ppb sensitivity). Only solutions that showed negative results were used for extractions. Mass balance of Fe(II) was calculated by comparing the sum of all independently measured Fe(II) species with the total Fe(II) as measured by 0.5 N HCl. The mass balance was reasonably good (92% or better).

Preparation of Fe(III)-reduced NAu-2 for Tc(VII) reduction

Once the Fe(II) concentration had leveled off, the Fe(III) bioreduction experiments were stopped by means of pasteurization (at 80ºC for 3 h). The extent of bioreduction was measured by means of 0.5 N HCl extraction. The bioreduced NAu-2 was washed four times in anaerobic, sterile, DI water to remove lactate and anthraquinone-2, 6-disulfonate (AQDS) by centrifugation and re-suspended in the same solution. The amount of lactate and AQDS remaining in the final wash was measured using high-performance liquid chromatography (HPLC). The remaining lactate was found to be ~4 μmol/g of NAu-2 and AQDS was not detectable. The amount of buffer remaining after washing should be =0.1 μmol/L. The concentration of the NAu-2 suspension was measured by drying an aliquot of the suspension for 72 h at 65ºC.

Chemically reduced (for 5 days) NAu-2 samples were also prepared by washing four times with anaerobic, sterile, DI water to remove any residual dithionite (Liu *et al.*, 2005). The extent of total Fe(III) reduction, Fe(II) partitioning, and final NAu-2 concentration were measured as above.

Tc(VII) reduction experiment

$Tc(VII)O_4^-$ reduction experiments were performed using both biologically and chemically reduced NAu-2 at different extents at pH 7.0. The Tc stock solution was in the form of $NH_4Tc(VII)O_4$. All experiments were performed in 20 mL glass vials inside a glove box. The glass vials were capped with thick butyl rubber stoppers and crimp sealed. The experiment vials were hand-shaken carefully once a day, to mimic natural conditions. At different time intervals, the Tc-NAu-2 suspension was sampled with a syringe using anaerobic techniques. The suspension sample was centrifuged to obtain soluble Tc, which was operationally defined as Tc(VII). The Tc(VII) activity in the filtrate was measured by liquid scintillation counting (Beckman LS8100), which was later converted to the Tc concentration using a standard Tc activity-concentration relationship (Fredrickson *et al.*, 2004). The time-course decreases in Fe(II) species in different reactive sites as a result of Tc reduction were measured.

Reactivity of different Fe(II) species in terms of Tc(VII) reduction

To determine the reactivity of the various Fe(II) species associated with NAu-2 [$Fe(II)_{acetate}$, $Fe(II)_{NH_4Cl}$, and $Fe(II)_{str}$ (Na-acetate extractable, NH_4Cl-extractable, and structural Fe(II), respectively] in terms of Tc(VII) reduction, three types of NAu-2 samples were prepared: (1) Fe(II) mainly at the surface complexation ($\equiv$SOH) sites, prepared by sorbing 60 μmol Fe(II)/g of unreduced NAu-2 in a strictly anaerobic environment in a glove box (monitored by CHEMets® colorimetric analysis kit R-7540) (Bradbury and Baeyens, 1997); (2) Fe(II) in all reactive sites of reduced NAu-2 (33.5% and 35% Fe(III) reduction for biologically and chemically reduced NAu-2, respectively); and (3) Fe(II) presumably at the structural sites only, prepared by removing $Fe(II)_{acetate}$ and $Fe(II)_{NH_4Cl}$ species from the same stock of reduced NAu-2 with the Na acetate (pH 4.25) and ammonium chloride (pH 7), respectively (see above). These samples with Fe(II) in different reactive sites were reacted individually with 60 μmol/L of Tc(VII) at pH 7.0 and the time-course change in Tc(VII) concentration was measured. We did not measure the reactivity of $Fe^{2+}_{(aq)}$, as it was analyzed in detail by Zachara *et al.* (2007).

In order to understand the effect of the interlayer cation composition on the electron-transport process, the reduced NAu-2 consisting of $Fe(II)_{str}$ only (after removing the $Fe(II)_{acetate}$ and $Fe(II)_{NH_4Cl}$ species) was

homo-ionized in Na and K (following the same procedure as for the unreduced sample, but in an anaerobic environment). To eliminate the steric effect due to different extents of reduction and dilution, the post-reduction homo-ionization (in Na and K) of reduced NAu-2 was prepared from the same stock solution as that used for examination of Fe(II)-species reactivity (see above). The time-course Tc(VII) reduction was measured as before. Again, these homoionized, reduced NAu-2 samples were analyzed by XRD to verify the collapsed interlayer spacing.

RESULTS

Fe(II) partitioning as a function of the extent of Fe(III) reduction

Various extents of Fe(III) reduction in NAu-2, ranging from 1.2% to 71%, were achieved *via* chemical reduction. The concentration of $Fe^{2+}_{(aq)}$ increased consistently with increasing extent of reduction (Figure 1a); however, it constituted only a small fraction (<5%) of total Fe(II). Similarly, the concentration of $Fe(II)_{acetate}$ consistently increased as the extent of Fe(III) reduction increased (Figure 1b) and attained the maximum value at 40−45% of Fe(III) reduction. For any further increase in the extent of reduction, the maximum concentration of $Fe(II)_{acetate}$ remained nearly constant. The concentration of the $Fe(II)_{acetate}$ in NAu-2 was ~60 μmol/g (*i.e.*120 meq/kg), which was reasonably close to the surface-site concentration of ≡SOH (141 meq/kg) in NAu-2 (measured independently by a potentiometric titration method, Jaisi *et al.*, 2007; authors' unpublished results).

The concentration of the $Fe(II)_{NH_4Cl}$ species was very small (<2%) at the limited extents of reduction (~20% or less). With increasing Fe(III) reduction and Fe(II) production, the proportion of Fe(II) partitioned into these sites increased. The concentration of $Fe(II)_{NH_4Cl}$ increased dramatically once the $Fe(II)_{acetate}$ reached saturation at ~45% Fe(III) reduction (Figure 1c). After that, $Fe(II)_{NH_4Cl}$ slowly but steadily increased with additional Fe(III) reduction. The maximum concentration of $Fe(II)_{NH_4Cl}$ was found to be close to the CEC of native NAu-2 (*i.e.* 697.1 (±73.4) meq/kg, Jaisi *et al.*, unpublished results). However, as the CEC increases with increased extent of Fe(III) reduction (Shen and Stucki, 1994; Stucki *et al.*, 2002; Favre *et al.*, 2006), the exchange sites may contain other cations (which originally existed at the interlayer or those produced *via* dissolution).

Fe(II) at structural sites ($Fe(II)_{str}$), *i.e.* Fe(II) species that could not be extracted by the ammonium-chloride

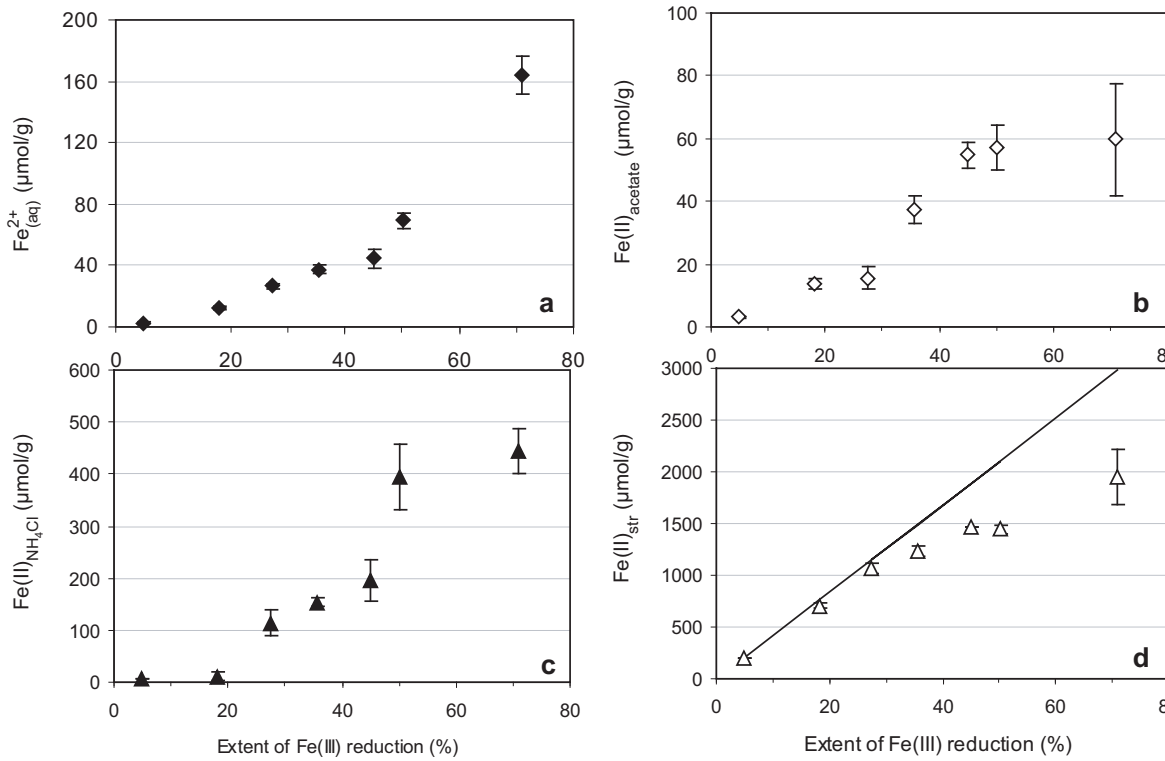

Figure 1. Fe(II) partitioning into different reactive sites as a function of Fe(III) reduction in NAu-2: aqueous Fe(II), *i.e.* $Fe^{2+}_{(aq)}$ (a); Fe(II) extracted by Na-acetate, presumed to be dominant at the surface complexation sites (b); Fe(II) extracted by NH_4Cl presumed to be dominant at the ion-exchangeable sites (c); and, structural Fe(II) (d). The straight line in (d) represents the amount of Fe(II) if all Fe(II) remained at the structural sites.

and Na-acetate methods, was close to 100% at low degrees of Fe(III) reduction (Figure 1d). When the extent of reduction was >~30% (although there was a gradual transition), NAu-2 dissolution occurred with a consequent release of Fe(II) from the structural sites. The dissolved Fe(II) released, partitioned into the surface-complexation sites, exchangeable sites, and aqueous solution. As a result, a corresponding decrease in the $Fe(II)_{str}$ concentration was observed. For example, at 50% Fe(III) reduction, the relative proportions of $Fe^{2+}_{(aq)}$, $Fe(II)_{NH_4Cl\ cpx}$, $Fe(II)_{acetate}$, and $Fe(II)_{str}$ were 4%, 3%, 20%, and 73%, respectively. The mass balance of Fe(II) (a comparison between the sum of all Fe(II) species measured independently and total Fe(II)) was normally better than 92%.

NAu-2 dissolution as a function of Fe(III) reduction

A significant quantity of cations, especially Si, was released from the NAu-2 into the supernatant solution during Fe(III) reduction by both biological and chemical methods. Such a release was particularly pronounced when the extent of Fe(III) reduction was > ~25%. A significant amount of cations, however, was also observed in control experiments without any Fe(III) reduction (*i.e.* at time 0 in Figure 2). Whether certain cations were already present before Fe(III) reduction was not clearly understood. However, a limited amount of these cations was possibly produced from dissolution of any amorphous materials and/or impurities (carbonates/Fe oxides) in unreduced NAu-2 (Keeling *et al.*, 2000). Nonetheless, all cation concentrations increased with increasing Fe(III) reduction except for Al, the concentration of which decreased continuously with Fe(III) reduction. This odd Al dissolution behavior was consistent with a previous observation for dithionite-reduced smectite (Stucki *et al.*, 1984b).

The amount of NAu-2 dissolution measured, based on Si, a proposed indicator of smectite dissolution (Amran and Ganor, 2005), was 2.1% when the extent of biological Fe(III) reduction was 31%. Similarly, the extent of NAu-2 dissolution was 1.3% and 5.9% for NAu-2 that had been chemically reduced to 31% and 71%, respectively. Since silica normally supersaturates in aqueous solution at neutral pH (Furukawa and O'Reilly, 2007), the aqueous concentration of silica would normally underestimate the extent of clay dissolution, because precipitated and other surface-bound Si forms were not accounted for in the measurement of aqueous Si. Fe(II) could be another indicator to approximate the extent of NAu-2 dissolution, especially when all Fe(II) species were measured in this study. Based on the amount of structural Fe(II) remaining (Figure 1d), the extent of Fe(II) dissolution (out of the NAu-2 structure) was ~35% at 71% extent of Fe(III) reduction (for chemical reduction). The amount of NAu-2 dissolution at other extents of Fe(III) reduction is reported in Table 1.

0.5 N HCl extraction efficiency and crystallinity of reduced NAu-2

The measurement of total Fe(II) produced during bioreduction of clay minerals and clay-rich sediments (by 0.5 N HCl extraction followed by Ferrozine assay) was previously reported to underestimate the extent of Fe(III) reduction. The variations reported in the literature were: ~27% in nontronite (NAu-2) (Jaisi *et al.*,

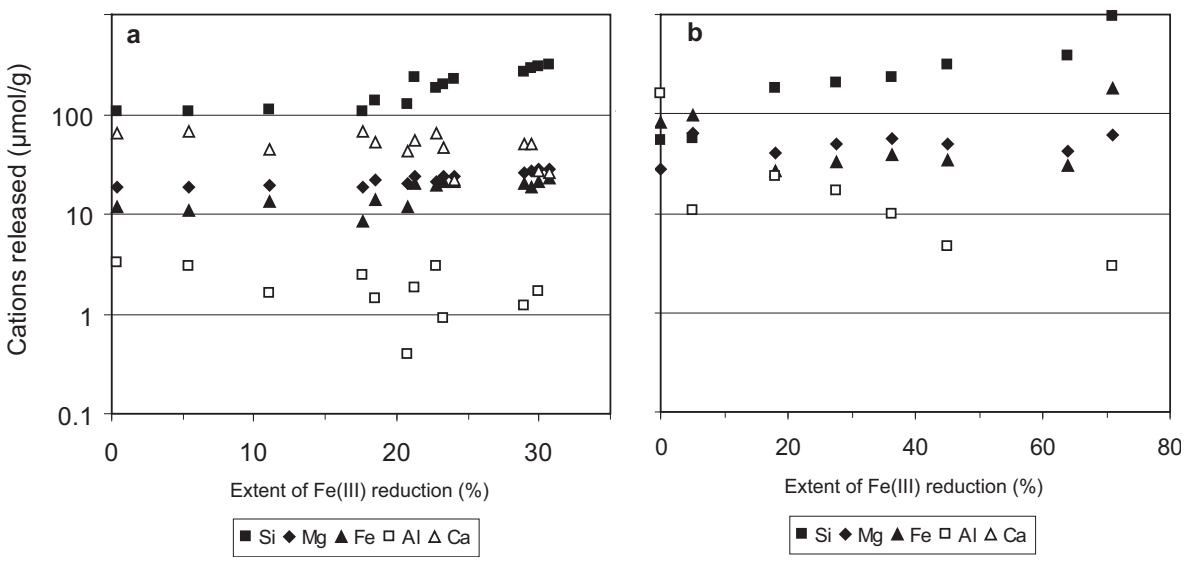

Figure 2. Reductive dissolution of major structural cations during (a) biologically mediated and (b) chemical Fe(III) reduction. The cation concentrations were measured by the direct current plasma (DCP) method. The cation concentrations at 0% Fe(III) reduction correspond to controls.

Table 1. XRD pattern characteristics, solution chemistry, layer charge, and extent of dissolution as a function of Fe(III) reduction.

Extent of Fe(III) reduction (%)	Relative peak intensity[1]	Peak shift °2θ[2]	Relative FWHM[1]	Increase in ionic strength (meq/L)[3]	Layer charge (e^-/unit cell)[4]	Extent of dissolution based on Fe(II)[5]
Chemical reduction (by dithionite)						
0	1.00	0.00	1.00	0.00		0.00
7	1.15	0.00	0.72	−1.28		2.01
17	0.66	0.10	1.01	0.77		7.09
29	0.63	0.10	0.78	1.27		14.12
40	0.51	0.13	1.44	1.78		19.98
54	0.25	0.12	1.50	3.56		31.56
71	0.15	0.90		15.99		34.61
Biological reduction (by CN32 cells)						
0	1.00	0.00	1.00	0.00	0.47	0.00
9	0.75	0.05	1.18	0.00		2.15
15	0.66	0.30	1.45	0.00		5.31
21	0.64	0.32	1.55	1.62		5.21
31			1.64	3.94	0.61	12.57

[1] Peak intensity and full width at half maximum (FWHM) was calculated relative to native NAu-2 FWHM is a measure of the broadness of peak.
[2] Shift of the 001 peak was compared to native NAu-2. The native (control) had a 001 peak at 17.8 Å and 15.6 Å in biologically and chemically reduced NAu-2, respectively.
[3] Change in ionic strength (of soluble ions) compared to control experiments
[4] Results from Jaisi *et al*. (2005)
[5] Percent calculated from the dissolved cations originally present in the NAu-2 structure

2007b); 2% in ferruginous smectite (SWa-1) (Kostka *et al.*, 1996); and 10% in clay-rich sediments (Cooper *et al.*, 2000). In our previous study (Jaisi *et al.*, 2007b), when comparing the extent of Fe(III) bioreduction by 0.5 N HCl extraction and by total HF acid dissolution, the greatest degree of Fe(III) reduction achieved was ~52%. The measured decrease in the concentration of structural Fe(II) with an increased degree of Fe(III) reduction (Figure 1d) prompted us to extend this comparison to greater degrees of Fe(III) reduction. Because the extent of Fe(III) bio-reduction was limited to ~35% (under 0.5 N HCl extraction), or to 52% (under acid dissolution) (Jaisi *et al.*, 2005, 2007b), we made such a comparison using chemically reduced NAu-2 samples. A plot of Fe(II), measured by the HF total dissolution method (Andrade *et al.*, 2002) *vs*. the 0.5 N HCl extraction followed by Ferrozine assay (Fredrickson *et al.*,1998; Zachara *et al.*, 1998; Stookey, 1970), showed that the disparity between these two methods was greater with small amounts of Fe(III) reduction (Figure 3). This disparity decreased as the extent of Fe(III) reduction increased and became negligible when the extent of reduction was great (*i.e*. ~60% or more) (Figure 3). This result suggested that the efficiency of 0.5 N HCl at extracting Fe(II) was a function of Fe(III) reduction.

To understand the change in crystallinity of NAu-2 as a result of Fe(III) reduction, XRD patterns of both chemically and biologically reduced NAu-2 were obtained (Figure 4, Table 1). No significant change in peak intensity or peak width was observed for the biologically reduced NAu-2 (up to 21% reduction). These results suggested that the crystallinity of NAu-2 was not significantly different from that of unreduced NAu-2, as consistent with a small amount of dissolution (~5%, Table 1). The XRD results showed a small but systematic shift in the 001 peak position with increase in the extent of Fe(III) bioreduction (Figure 4a). For example, the 2θ angle increased from 4.96 to 5.2°

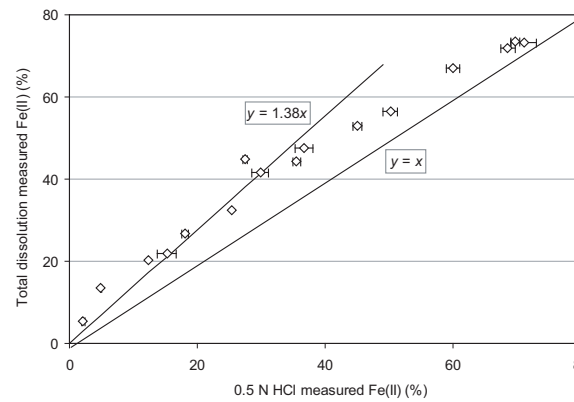

Figure 3. Relationship between the Fe(II) concentration as measured by 0.5 N HCl extraction followed by the Ferrozine method and that as measured by HF total dissolution and titration.

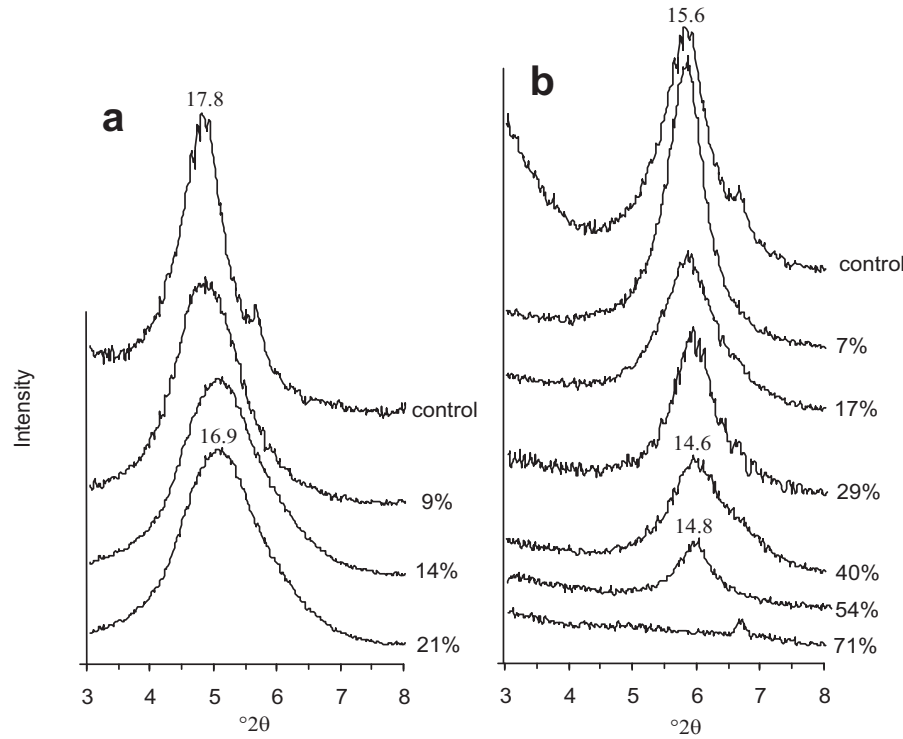

Figure 4. XRD pattern showing the 001 peak for differentially reduced NAu-2: (a) biologically mediated Fe(III) reduction; and (b) chemical Fe(III) reduction. The values given in the XRD spectra are *d* spacings (Å).

(corresponding to a decrease in the interlayer spacing from 17.8 to 16.9 Å) when the extent of reduction increased from negligible levels to 21%. The ionic strength of the aqueous solution was approximately constant in all bioreduction experiments, except for a small contribution from reductive dissolution of NAu-2 (=1.62 meq/L, Figure 2 and Table 1). Such a small shift in *d* spacing was consistent with the change in ionic strength of the solution. No significant change in peak intensity or peak width was observed for the range of Fe(III) reduction tested. These results suggested that the crystallinity of biologically reduced NAu-2 was not significantly altered.

In contrast, the chemically reduced samples showed a systematic decrease in the 001 peak intensity with an increased extent of Fe(III) reduction. The 001 peak became progressively broader with increased Fe(III) reduction and ultimately appeared X-ray amorphous when the extent of Fe(III) reduction reached 71% (Figure 4b). However, the 001 peak position remained nearly constant, except for the greatest degree of reduction (see discussion). Such a change in NAu-2 crystallinity was consistent with a large amount of NAu-2 dissolution (35%) (Table 1). Additionally, the approximate agreement by the 0.5 N HCl extraction and HF dissolution in estimating the extent of Fe(III) reduction, at greater extents of Fe(III) reduction, further implied that crystallinity of residual NAu-2 decreased progressively with increased extent of Fe(III) reduction.

Effect of interlayer cation on Fe(III) bioreduction

In the identically treated samples, the extent of Fe(III) reduction in the Na-NAu-2 (homoionic in Na) was consistently greater than that in the K-NAu-2 (homo-ionic in K) at each time point (Figure 5). This result was consistent in both types of treatments (with and without AQDS). For example, in 202 days, the extent of reduction reached 8.6% and 25.3% in the absence and presence of AQDS, respectively, in the case of Na-NAu-2. Over the same period, the extent of reduction was 7.1% and 19.5% in the absence and presence of AQDS, respectively, for K-NAu-2. After 7.2 days of incubation, the extent of Fe(III) reduction was 16% and 33% greater in the Na-NAu-2 than that in the K-NAu-2 in the absence and presence of AQDS, respectively.

Sodium and K have been reported to inhibit growth of *Shewanella oneidensis* MR-1 (Katz and Hazen, 2005) with 50% growth inhibition at 250 and 6000 ppm of Na and K, respectively, suggesting that Na was more effective than K at inhibiting cell growth. Our experiments were performed at a greater Na concentration than this limit (250 ppm) in order to maintain adequate buffering capacity (Dong *et al.*, 2003a, 2003b; Kim *et al.*, 2004; Li *et al.*, 2004; Jaisi *et al.*, 2005). If we assume that the same inhibition mechanism operated in our experiments, Na-NAu-2 would be the one to exhibit the inhibitory effect, not K-NAu-2. Our data did not support this explanation, however, but instead showed the

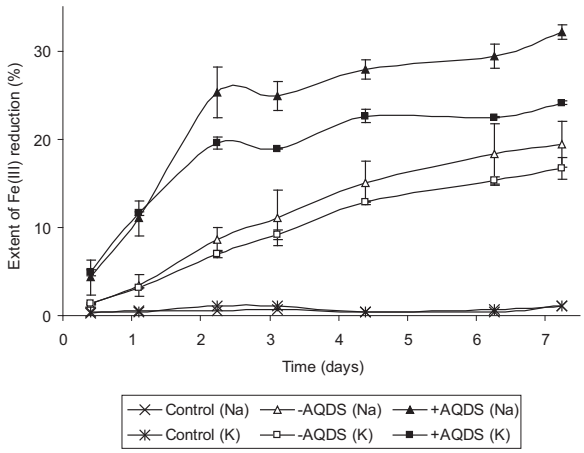

Figure 5. Microbial reduction of Fe(III) in Na-NAu-2 (homoionic in Na) and K-NAu-2 (homoionic in K). The samples were treated identically and the experiments were performed in 30 mM of PIPES buffer. The XRD patterns of homoionic NAu-2 were collected in order to verify collapsed interlayer spacings (data not presented).

opposite result. Therefore, it is very likely that the interlayer cation (K or Na) and its hydration shell may have affected the electron-transport process (see discussion below).

Overall reactivity of reduced NAu-2 in terms of Tc(VII) reduction

The reactivity of NAu-2 chemically reduced from 4.5% to 44.5% was used to identify whether the total concentration of Fe(II) influenced Tc(VII)O_4^- reduction. As expected, the rate and extent of Tc(VII) reduction was proportional to the extent of Fe(III) reduction (*i.e.* total Fe(II) concentration) in NAu-2. For example, chemically reduced NAu-2 with the greatest extent of Fe(III) reduction (*i.e.* largest Fe(II) concentration) exhibited the greatest rate and extent of Tc reduction (Figure 6a). However, when Tc(VII) reduction was normalized to the product of NAu-2 mass and Fe(II) concentration, all four curves converged reasonably during the main phase of Tc(VII) reduction (Figure 6b). This result suggested that both NAu-2 and total Fe(II) concentrations were primarily responsible for controlling the Tc(VII)-Fe(II) interaction.

Reactivity of different Fe(II) species in terms of Tc(VII) reduction

The overall reactivity of Fe(II) and individual reactivities of $Fe(II)_{acetate}$ and $Fe(II)_{str}$ (from 33.5 and 35% Fe(III) reduction in biologically and chemically reduced NAu-2, respectively) were compared in Figure 7. To account for the Fe(II) and NAu-2 concentration effects, the observed reactivity was normalized by dividing the cumulative Tc(VII) reduction by the product of NAu-2 mass and initial Fe(II) concentration (same as Figure 6b). The reactivity of the sorbed Fe(II) mainly at surface complexation sites was the greatest among all Fe(II) species present, suggesting that the surface-complexed Fe(II) was the most reactive in terms of Tc(VII) reduction. Although the concentration of sorbed Fe(II) (60 μmol/g) was slightly less than the independently measured ≡SOH site concentration in NAu-2 (141 meq/g), it was equal to that measured by Na acetate extraction.

When Fe(II) was present in all reactive sites, the overall reactivity was less than that of the $Fe(II)_{acetate}$ alone. The measured partitioning of $Fe^{2+}_{(aq)}$, $Fe(II)_{acetate}$, and $Fe(II)_{NH_4Cl}$ at these extents of Fe(III) reduction (*i.e.* 33.5% and 35% for biologically and chemically reduced NAu-2) was ~34, 25, and 150 μmol/g, respectively (Figure 1). This result suggests that the overall reactivity was also contributed by the $Fe(II)_{str}$. When $Fe(II)_{str}$ was present alone, a certain degree of reactivity in terms of

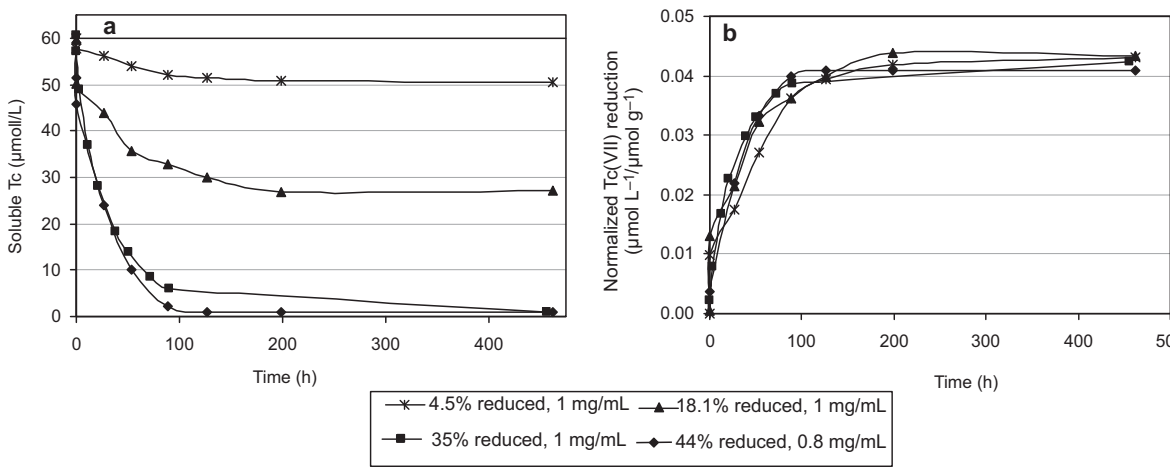

Figure 6. (a) Tc(VII) reduction as a function of Fe(II) concentration in NAu-2 which was initially reduced to different extents by dithionite. (b) Normalized Tc(VII) reduction (relative to NAu-2 mass and Fe(II) concentration) with time. The data were taken from (a).

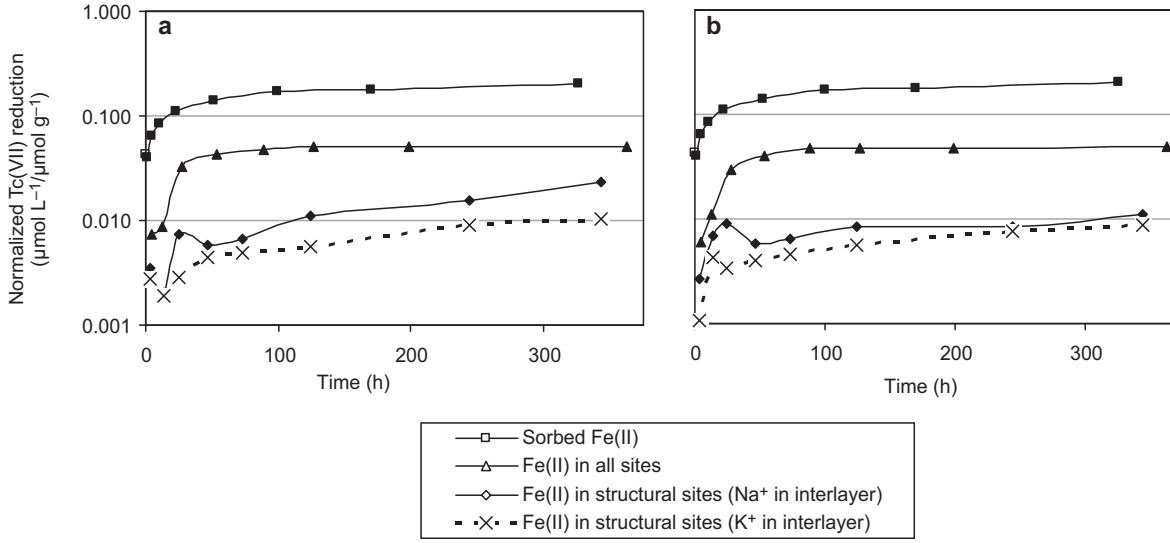

Figure 7. Normalized Tc(VII) reduction by Fe(II) species associated in different reactive sites in (a) biologically, and (b) chemically reduced NAu-2. The original Tc(VII) at $t = 0$ was 60 μmol/L. For the biologically reduced samples, the total concentrations of Fe(II) and structural Fe(II) were 1264 μmol/L and 400 μmol/L, respectively. Similarly, the total concentrations of Fe(II) and structural Fe(II) were 1498 and 373 μmol/L, respectively, in the chemically reduced samples. The concentration of Fe(II) sorbed primarily at the surface complexation sites was 60 μmol/L (shown in both treatments). The K-homoionic, reduced NAu-2 samples were verified by collapsed, 10 Å layer spacing on XRD patterns (not shown).

Tc(VII) reduction was also observed (Figure 7). The reactivity of $Fe^{2+}_{(aq)}$ was not determined as it was recently analyzed in detail (Zachara *et al.*, 2007). Their results showed that the reactivity of $Fe^{2+}_{(aq)}$ was large when $Fe^{2+}_{(aq)}$ gradually sorbed onto newly precipitated hydrous ferric oxide.

Effect of interlayer cation on reactivity of structural Fe(II)

To assess the effect of the interlayer composition on the electron-transport process, K and Na homoionized, reduced NAu-2 (consisting of structural Fe(II) only) was reacted with $Tc(VII)O_4^-$ (Figure 7). The reactivity of structural Fe(II) in the K-exchanged NAu-2 was less than that in the Na-exchanged NAu-2 for both chemically and biologically reduced NAu-2, when the concentration of Fe(II) was kept constant. This relative order of Tc(VII) reactivity between K- and Na-homoionized NAu-2 (Figure 7) was consistent with the relative extent of Fe(III) reduction (Figure 5).

DISCUSSION

Change of structural integrity of NAu-2 with increased Fe(III) reduction

Our data collectively demonstrated that the integrity of the nontronite structure was an inverse function of the extent of Fe(III) reduction. When the extent of Fe(III) reduction was small (<~30%), the nontronite structure largely remained intact, as shown by ~100% retention of biogenic Fe(II) in the structure (Figure 1d), incomplete extraction by 0.5 N HCl (Figure 3), and nearly constant breadth of the 001 peak of NAu-2 in the XRD pattern (Figure 4a). These results suggested that solid-state Fe(III) reduction (Manceau *et al.*, 2000a, 2000b; Lee *et al.*, 2006) was only possible when the extent of Fe(III) reduction was small (<30%). These reduced NAu-2 samples were expected to restore to unreduced conditions upon reoxidation, as documented by Lee *et al.* (2006) for Garfield nontronite samples with ~20% Fe(III) reduction. Our data demonstrated this relationship consistently.

When the extent of Fe(III) reduction increased further (> 30%), the nontronite structure apparently became less stable or even became partly X-ray amorphous as shown by the nearly complete extraction of Fe(II) by 0.5 N HCl (Figure 3), <100% retention of Fe(II) in the structure sites (Figure 1d), and significant broadening of the 001 peak in the XRD pattern of reduced NAu-2 (Figure 4b, Table 1). A certain portion of NAu-2 must have dissolved at this stage, as shown by release of structural Fe(II) (Figure 1d). At this stage, the nontronite structure may no longer be able to accommodate all Fe(II). The replacement of Fe(III) by Fe(II) in the structure may create local instability in the Fe sites and thus provides a basis for structural rearrangements that may provoke dissolution of Fe and Si (Stucki *et al.*, 1984b; Fialips *et al.*, 2002). These results are consistent with those of several previous studies (Dong *et al.*, 2003a, 2003b; Li *et al.*, 2004; Kim *et al.*, 2004; Jaisi *et al.*, 2005, 2007b) in showing that the nontronite structure dissolves as a result of Fe(III) bioreduction.

In spite of these independent and consistent results suggesting reductive dissolution of NAu-2, the extent of dissolution could not be quantified due to multiple

complications such as incongruent dissolution of the nontronite structure and variable partitioning and solubility of released major elements such as Si, Al, Fe, and Ca. Assuming Si release as a possible indicator of dissolution as previously assumed (Amran and Ganor, 2005), the extent of dissolution was limited to only 5.9% at the greatest degree of reduction (71% level of chemical reduction). This amount of dissolution was far less than that reported by Rozenson and Heller-Kallai (1976) in unbuffered nontronite solutions (~20%), but was slightly greater than that reported by Stucki *et al.* (1984b) (0.4–4%) with the same chemical reductant (Na-dithionite). The greater extent of dissolution in our experiments than observed by Stucki *et al*. (1984b) was probably related to occupancy of Fe(III) in the tetrahedral sites of NAu-2 (Gates *et al.*, 2002), as opposed to ferruginous smectite and nontronite used in the Stucki *et al.* (1984b) study. The tetrahedral occupancy of Fe(III) and its greater reducibility (among tetrahedral, *trans*- and *cis*-octahedral Fe(III)) (Cardile and Slade, 1987; Jaisi *et al.*, 2005) might have promoted more extensive dissolution.

The estimation of the extent of dissolution by measuring silica released in the solution may not be very reliable given the fact that Si precipitates at neutral pH (Furukawa and O'Reilly, 2007). Since we measured each Fe(II) species in differentially reduced NAu-2 and the mass balance was normally better than 92%, the extent of dissolution could be estimated more reliably from the amount of Fe(II) that was not retained in the structure (Figure 1d). According to this approach, there was 35% Fe(II) dissolution at 71% of Fe(III) reduction, a significantly larger number than that estimated based on aqueous Si concentration. It should be cautioned, however, that neither Si nor Fe is a perfect measure of dissolution, given the complications of incongruent dissolution, sorption and solubility issues of NAu-2, and any secondary mineral precipitation.

It was important to note that despite the extensive changes to the NAu-2 structure at significant degrees of Fe(III) reduction (>30%), the 001 peak position (and thus interlayer spacing) was apparently constant (Figure 4) (except removal of two or one layers of water in biologically and chemically reduced NAu-2, respectively). Such invariant layer spacing may be a result of the coexistence of fully collapsed, partially expanded, and fully expanded layers in the same crystallite of reduced NAu-2 (Foster *et al.*, 1955; Rhoades *et al.*, 1969; Viani *et al*., 1983; Wu *et al.*, 1989). The observed insensitivity of the interlayer spacing to the extent of Fe(III) reduction also appeared to be consistent with the explanation by Lear and Stucki (1989) that some of the layers did actually collapse but they were so randomly interstratified that they were not detectable by XRD. Another possibility might be related to increased Na concentration (due to high Na-dithionite concentration required to reduce more Fe(III)). As a result, the limited amount of Fe(II) produced may not be able to replace completely the Na in the ion-exchangeable sites due to the mass effect, even though the selectivity coefficient of Fe is greater than that of Na (Baeyens and Bradbury, 1997).

Partitioning of Fe(II) into reactive sites

Fe(II) partitioning was found to vary as a function of the extent of Fe(III) reduction. At small degrees of Fe(III) reduction, the $Fe(II)_{str}$ accounted for nearly 100% of total Fe(II). Therefore, the measured Fe(II) in non-structural sites (Figure 1a–c) was probably due to the presence of impurities (Keeling *et al.*, 2000) or to unknown amorphous Fe(II) phases in the unreduced NAu-2. The presence of other aqueous cations, even in the abiotic control, or at very small degrees of Fe(III) reduction (Figure 2) also suggested some contribution from soluble or amorphous materials. This difficulty was also reported by Baeyens and Bradbury (1997). These authors noted that it was almost impossible to remove all impurities in clay minerals. Although our extensive XRD, scanning electron microscopy (SEM) with energy dispersive spectroscopy (EDS), and Mössbauer spectroscopy (Jaisi *et al.*, 2005) did not identify any impurities, Keeling *et al*. (2000) reported very small (~1%) amounts of impurities in NAu-2. The presence of these impurities may have some effect on partitioning of Fe(II) species. However, given several other uncertainties (such as inter-species Fe(II) transfer (Jaisi *et al.*, unpublished results) and possible inter-valence Fe(II)-Fe(III) electron transfer (Lear and Stucki, 1987; Williams and Scherer, 2004), any effects from trace impurities would be minimal and therefore we ignored them in this study.

At larger degrees of reduction (>30%), $Fe(II)_{str}$ was released and partitioned into different reactive sites, according to the relative affinity of these sites for Fe(II). For example, increase in $Fe(II)_{acetate}$ during the early stage of Fe(III) reduction suggested that the surface complexation sites were the most favored Fe(II) sorption sites, although the concentration of such sites was relatively small in NAu-2 (~141 meq/kg). Subsequent increase in $Fe(II)_{NH_4Cl}$ concentration suggested that the ion-exchangeable sites were the second most preferred sites for Fe(II), as Fe(II) could progressively replace interlayer Na due to its greater selectivity constant (Baeyens and Bradbury, 1997). The rate at which Fe(II) partitioned into the ion-exchangeable sites accelerated once the surface complexation sites were partially or fully saturated. Eventually, the Fe(II) concentration at the ion-exchangeable sites slowly reached the CEC value of native NAu-2 (at ~55–60% Fe(III) reduction) (Figure 1b), beyond which point any further Fe(II) released from the nontronite structure would occur as $Fe^{2+}_{(aq)}$. Since the CEC would increase continuously and steadily due to Fe(III) reduction (Stucki *et al.*, 1984b; Shen and Stucki, 1994), the amount of Fe(II) at the ion-exchangeable sites may not accurately reflect the CEC

value of native NAu-2, but instead reflect the CEC value of reduced NAu-2. Additional complexities may have existed; *e.g.* other cations released from reductive dissolution of NAu-2 (Figure 2) would also be available to exchange with the interlayer cations. Some cations (such as Si, Al) having greater selectivity coefficients than that of Fe(II) could replace Fe(II) in the ion-exchangeable sites. Therefore, actual interlayer cation composition (both fixed and exchangeable) might be more than just Fe, although concentration of other cations was expected to be insignificant (Figure 1).

Bulk reactivity of reduced NAu-2 in terms of Tc(VII) reduction

The dependency of Tc(VII) reduction on the extent of Fe(III) reduction in NAu-2 was due to the Fe(II) concentration effect, since more Fe(II) was produced at greater degrees of Fe(III) reduction. When the Fe(II) concentration effect was accounted for by normalizing the extent of Tc(VII) reduction by the product of NAu-2 mass and Fe(II) concentration, all results showed a nearly identical trend (Figure 6b). It strongly suggested that the reactivity (*i.e.* $Tc(VII)O_4^-$ reduction activity) was a function of Fe(II) concentration. This result, however, may not be true in later phases of the experiments, because of the formation and accumulation of $TcO_2{\cdot}nH_2O$. Continued oxidation of Fe(II) would inhibit additional Tc(VII) reduction, probably due to passivation from precipitated Fe(III) hydroxides (Brusic, 1972; Morrison, 1980).

The overall rate of Tc(VII) reduction by Fe(II) in NAu-2 (after normalization to total Fe(II) concentration) was greater than that by sediment-associated Fe(II) in Hanford saprolite (Fredrickson *et al.*, 2004), but less than that by Fe(II) associated with Fe oxides (Cui and Erickson, 1996). The rate of Tc(VII) reduction by bacteria was very dependent on solution chemistry (Wildung *et al.*, 2000) and hence could not be compared with an abiotic reduction rate. These data have important implications for field-scale applications, where the Tc(VII) reduction rate is to be maximized.

Reactivity of different Fe(II) species in terms of Tc(VII) reduction

Our data (Figure 7) suggest that the Fe(II) species at the surface-complexation sites (*i.e.* $Fe_{acetate}$) was the most reactive among all Fe(II) species. This is consistent with previous findings that the Fe(II) adsorbed on surfaces of different minerals was the most reactive for a number of inorganic and organic contaminants (Morris *et al.*, 1990; Buerge and Hug, 1999; Amonette, 2003; Chisholm-Brause *et al.*, 1994; Elsner *et al.*, 2004; Silvester *et al.*, 2005). This reactivity of surface-complexed Fe(II) may be understood in terms of the surface-complexation theory. The hydroxo ligands favor oxidation of Fe(II) by effectively releasing electrons due to its high electron density and corresponding generation of more stable Fe(III) (Stumm and Morgan, 1996; Luther *et al.*, 1996).

When all Fe(II) species were present, it is not clear if $Fe(II)_{NH_4Cl}$ contributed to the overall extent of Tc(VII) reduction. A limited amount of Fe(II) as $Fe(II)_{acetate}$ (~20 μmol/g) would have been exhausted early during the Tc(VII) reduction. Therefore, unless $Fe(II)_{NH_4Cl}$ and/or $Fe(II)_{str}$, or both, participated in the Tc(VII)-Fe(II) redox reaction, there would not have been any additional Tc(VII) reduction.

The structural Fe(II) was found to be a less reactive species than the surface-complexed Fe(II). It reduced Tc(VII) to a moderate degree when NAu-2 consisted of structural Fe(II) species only. The apparent, small reactivity of structural Fe(II) may have resulted from its inaccessibility (due to its location) and bonding environment. Additionally, NAu-2 surface passivation, due to Fe(III) accumulation/ferrihydrite formation, or sorption/precipitation $Tc(IV)O_2{\cdot}nH_2O$ at surface sites might have resulted in decreased reactivity. The surface passivation has been found to be responsible for the large amount of residual Fe(II) when there was a large degree of Tc(VII) reduction and Fe(II) oxidation (Jaisi *et al.*, unpublished data).

In summary, our data showed that the surface-complexed Fe(II) was more reactive than the exchangeable or structural Fe(II). Our data did not allow us to determine the relative reactivity between the exchangeable and structural Fe(II). This result was qualitatively consistent with those reported by Hofstetter *et al.* (2003, 2006). Those authors reported that both surface complexed and structural Fe(II) were reactive in terms of reduction of nitroaromatic compounds, but the reactivity of interlayer Fe(II) was insignificant.

Role of interlayer expansion in Tc(VII) reduction

The reduction of Fe(III) in smectites can cause more K fixation in the interlayer sites than other cations (such as Ca, Cu, and Zn) (Khaled and Stucki, 1991; Shen and Stucki,1994), resulting in expulsion of interlayer water (Sposito and Post, 1982) and collapse of interlayer spacing, largely due to the small hydration energy of K relative to Na and other cations (Haderlein *et al.*, 1996; Weissmahr *et al.*, 1996). The layer collapse originates from the increased attractive force between clay layers of reduced smectite (Stucki and Huo, 1996). Conversely, any smectite/nontronite that is prefixed with K would retain collapsed and dehydrated interlayers. Such collapsed interlayers would make electron transfer more difficult, thus lowering the extent of Fe(III) reduction (Figure 5). Similarly, for Fe(II) species in the structure of NAu-2 that was pre-fixed with K, it would be more difficult to deliver electrons to Tc(VII), thus lowering the extent of Tc(VII) reduction (relative to Na) (Figure 7). Such interlayer hydration/collapses have been found to be key factors in controlling electron transfer (Ilton *et al.*, 1997, 2004; Amonette and Scott,

1995; Scott and Amonette, 1988), because Fe(III) reduction in smectites has been found to proceed from basal surfaces rather than from particle edges (Komadel *et al.*, 2006; Hofstetter *et al.*, 2006). Decreased reactivity of K-substituted smectite has been reported in the reduction of uranyl by ferrous mica (Ilton *et al.*, 2004), and reduction of chromate by a variety of clay minerals (Taylor *et al.*, 2000). All these results support the role of interlayer cations and hydration in controlling the rate of electron transfer (Cervini-Silva, 2004; Cervini-Silva *et al.*, 2006), suggesting that the layer collapse might have narrowed the possible electron-transfer pathways or partially blocked diffusion of redox reactive species into the interlayer.

ACKNOWLEDGMENTS

This research was supported by grants from the National Science Foundation (EAR-0345307) and the US Department of Energy (DE-FG02-07ER64369) to HD and by student research grants from The Clay Minerals Society (2006), Geological Society of America (2005), and the International Association of Mathematical Geology (2006) to DPJ. We are grateful to Will Gates and an anonymous reviewer for their constructive comments which greatly improved the quality of the manuscript.

REFERENCES

Albinsson, Y., Cristiansen-satmark, B., Engkvist, I., and Johansson, W. (1991) Transport of actinides and Tc through a bentonite backfilling containing small quantities of iron or copper. *Radiochimica Acta*, **52/53**, 283–286.

Amonette, J.E. (2003) Iron redox chemistry of clays and oxides: environmental applications. Pp. 89–148 in: *Electrochemical Properties of Clays* (A. Fitch, editor). The Clay Minerals Society, Aurora, Colorado, USA.

Ammonette, J.E. and Scott A.D. (1995) Oxidative weathering of trioctahedral micas by buffered H_2O_2 solutions. *Clays Controlling the Environment* (G.J. Churchman, editor). CSIRO Publishing, Melbourne, pp. 355–361.

Amran, K. and Ganor, J. (2005) The combined effect of pH and temperature on smectite dissolution rate under acidic conditions *Geochimica et Cosmochimica Acta*, **69**, 2535–2546.

Andrade, S., Hypolito, R., Ulbrich, H.H., and Silva, M.L. (2002) Iron(II) oxide determination in rocks and minerals. *Chemical Geology*, **182**, 85–89.

Baeyens, B. and Bradbury, M.H. (1997) A mechanistic description of Ni and Zn sorption on Na-montmorillonite. Part I: Titration and sorption measurements. *Journal of Contaminant Hydrology*, **27**, 199–222.

Bradbury, M.H. and Baeyens, B. (2002) Sorption of Eu on Na- and Ca-montmorillonites: Experimental investigations and modeling with cation exchange and surface. *Geochimica et Cosmochimica Acta* **66**, 2325–2334.

Bratu, C., Bratu, G., Galateanu, I., and Roman, M. (1975) Study of lower valence states of technetium. *Journal of Radioanalytical Chemistry*, **26**, 5–16.

Brusic, V. (1972) Passivation and passivity. Pp. 1–80 in: *The Anodic Behavior of Metals and Semiconductors Series* (J.W. Diggle, editor). Marcel and Dekker, Inc., New York.

Buerge, I.J. and Hug, S.J. (1999) Influence of mineral surfaces on chromium(VI) reduction by iron(II). *Environmental Science and Technology*, **33**, 4285–4291.

Bukka, K., Miller, J.D., and Shabtai, J. (1992) FTIR study of deuterated montmorillonites: Structural features relevant to pillared clay stability. *Clays and Clay Minerals*, **40**, 92–102.

Burke, I.T., Boothman, C., Lloyd, J.R., Mortimer, R.J.G., Livens, F.R., and Morris, K. (2005) Effects of progressive anoxia on the solubility of technetium in sediments. *Environmental Science and Technology*, **39**, 4109–4116.

Cantrell, K.J., Serne, R.J., and Last, G.V. (2003) *Hanford Contaminant Distribution Coefficient Database and Users Guide*. Pacific Northwest National Laboratory, Richland, Washington.

Cardile, C.M. and Slade, P.G. (1987) Structural study of a benzidine-vermiculite intercalate having a high tetrahedral-iron content by ^{57}Fe Mössbauer spectroscopy. *Clays and Clay Minerals*, **35**, 203–207.

Cataldo, D.A., Garland, T.R., Wildung, R.E., and Fellows, R.J. (1989) Comparative metabolic behaviour and interrelationships of Tc and S in soyabean plants. *Health Physics*, **57**, 281–288.

Cervini-Silva J. (2004) Coupled charge transfer- and hydrophilic-interactions between polychlorinated methanes, ethanes, and ethenes and redox-manipulated smectite clay minerals. *Langmuir*, **20**, 9878–9881

Cervini-Silva, J., Larson, R.A., and Stucki, J.W. (2006) Hydration/expansion and cation charge compensation modulate the Bronsted basicity of distorted clay water. *Langmuir*, **22**, 2145–2151.

Charlet, L., Silvester, E., and Liger, E. (1998) N-compound reduction and actinide immobilization in surficial fluids by Fe(II): The surface $=Fe^{III}OFe^{II}OH^{o}$ species, as major reductant. *Chemical Geology*, **151**, 85–93.

Chisholm-Brause, C., Conradason, S.D., Buscher, C.T., Eller, P.G., and Morris, D.E. (1994) Speciation of uranyl sorbed at multiple binding sites on montmorillonite. *Geochimica et Cosmochimica Acta*, **58**, 3625–3631.

Cooper, D.C., Picardal, F., Rivera, J., and Talbot, C. (2000) Zinc immobilization and magnetite formation via ferric oxide reduction by *Shewanella putrefaciens* 200. *Environmental Science and Technology*, **34**, 100–106.

Cui, D. and Eriksen, T. (1996) Reduction of pertechnetate in solution by heterogeneous electron transfer from Fe(II)-containing geological material. *Environmental Science and Technology*, **30**, 2263–2269.

Dong, H., Kostka, J.E., and Kim, J.W. (2003a) Microscopic evidence for microbial dissolution of smectite. *Clays and Clay Minerals*, **51**, 502–512.

Dong, H., Kukkadapu, R.K., Fredrickson, J.K., Zachara, J.M., Kennedy, D.W., and Kostandarithes, H.M. (2003b) Microbial reduction of structural Fe(III) in illite and goethite. *Environmental Science and Technology*, **37**, 1268–1276.

Elsner, M., Schwarzenbach, R.P., and Haderlein, S.B. (2004) Reactivity of Fe(II) bearing minerals towards reductive transformation of organic contaminants. *Environmental Science and Technology*, **38**, 799–807.

Favre, F., Bogdal, C., Gavillet, S., and Stucki, J.W. (2006) Changes in the CEC of a soil smectite-kaolinite clay fraction as induced by structural iron reduction and iron coatings dissolution. *Applied Clay Science* **34**, 95–104

Fialips, C.-I., Huo, D., Yan, L., Wu, J., and Stucki, J.W. (2002) Infrared study of reduced and reduced-reoxidized ferruginous smectite. *Clays and Clay Minerals*, **50**, 455–469.

Foster, W.R., Savins, J.G., and Waite, J.M. (1955) Lattice expansion and rheological behavior of relationships in water-montmorillonite systems. *Clays and Clay Minerals*, **395**, 296–316.

Fredrickson, J.K., Zachara, J.M., Kennedy, D.W., Dong, H., Onstott, T.C., Hinman, N.W., and Shu-mei, L. (1998) Biogenic iron mineralization accompanying the dissimila-

tory reduction of hydrous ferric oxide by a groundwater bacterium. *Geochimica et Cosmochimica Acta*, **62**, 3239–3257.

Fredrickson, J.K., Zachara, J.M., Kennedy, D.W., Kukadappu, R.K., Mckinley, J.P., Heald, S.M., Liu, C., and Plymale, A.E. (2004) Reduction of TcO_4 by sediment-associated biogenic Fe(II) *Geochimica et Cosmochimica Acta*, **68**, 3171–3187.

Furukawa, Y., and O'Reilly, S.E. (2007) Rapid precipitation of amorphous silica in experimental systems with nontronite (NAu-1) and *Shewanella oneidensis* MR-1. *Geochimica et Cosmochimica Acta*, **71**, 363–377

Gan, H., Bailey, G.W., and Yu, Y.S. (1996) Morphology of lead(II) and chromium(III) reaction products on phyllosilicate surfaces as determined by atomic force microscopy. *Clays and Clay Minerals*, **44**, 734–743.

Gates, W.P., Slade, P.G., Manceau, A., and Lanson, B. (2002) Site occupancies by iron in nontronites. *Clays and Clay Minerals*, **50**, 223–239.

Gates, W.P., Wilkinson, H.T., and Stucki, J.W. (1993) Swelling properties of microbially reduced ferruginous smectite. *Clays and Clay Minerals*, **41**, 360–364.

Giaquinta, D.M., Soderholm, L., Yuchs, S.E., and Wasserman, S.R. (1997) The speciation of uranium in a smectite clay: evidence for catalyzed uranyl reduction. *Radiochimica Acta*, **76**, 113–121.

Haderlein, S.B., Weissmahr, K.W., and Schwarzenbach, R.P. (1996) Specific adsorption of nitroaromatic explosives and pesticides to clay minerals. *Environmental Science and Technology*, **30**, 612–622.

Hess, N.J., Xia, Y., Rai, D., and Conradson, S.D. (2004) Thermodynamic model for the solubility of $TcO_2{\cdot}xH_2O$(am) in the aqueous Tc(IV)-Na^+-Cl^--H^+-OH^--H_2O system. *Journal of Solution Chemistry*, **33**, 199–226

Hofstetter, T.B., Neumann, A., and Schwarzenbach, R.P. (2006) Reduction of nitroaromatic compounds by Fe(II) species associated with iron-rich smectites. *Environmental Science and Technology*, **40**, 235–242.

Hofstetter, T.B., Schwarzenbach, R.P., and Haderlein, S.B. (2003) Reactivity of Fe(II) species associated with clay minerals. *Environmental Science and Technology*, **37**, 519–528.

Ilton, E.S., Haiduc, A., Moses, C.O., Heald, S.M., Elbert, D.C., and Veblen, D.R. (2004) Heterogeneous reduction of uranyl by micas: Crystal chemical and solution controls. *Geochimica et Cosmochimica Acta*, **68**, 2417–2435.

Ilton, E.S., Veblen, D.R., Moses, C.O., and Raeburn, S.P. (1997) The catalytic effect of sodium and lithium ions on coupled sorption-reduction of chromate at the biotite edge-fluid interface. *Geochimica et Cosmochimica Acta*, **61**, 3543–3563.

Jaisi, D.P., Kukkadapu, R.K., Eberl, D.D., and Dong, H. (2005) Control of Fe(III) site occupancy on the rate and extent of microbial reduction of Fe(III) in nontronite. *Geochimica et Cosmochimica Acta*, **69**, 5429–5440.

Jaisi, D.P., Dong, H., and Liu, C. (2007a) Analysis of Fe(III) reduction kinetics in nontronite. *Environmental Science and Technology*, **41**, 2434–2444.

Jaisi, D.P., Dong, H., and Liu, C. (2007b) Influence of biogenic Fe(II) on the extent of microbial reduction of Fe(III) in clay minerals nontronite, illite, and chlorite. *Geochimica et Cosmochimica Acta*, **71**, 1145–1158.

Katoh, S., Danhara, T., Hart, W.K., and Wolde-Gabriel, G. (1999) Use of sodium polytungstate solution in the purification of volcanic glass shards for bulk chemical analysis. *Natural Human Acta*, **4**, 45–54.

Katz, N. and Hazen, T.C. (2005) High throughput analysis of stress response in *Shewanella oneidensis* MR-1. (http://www.scied.science.doe.gov/scied/Abstracts2005/LBNLbio.htm)

Keeling, J.L., Raven, M.D., and Gates, W.P. (2000) Geology and characterization of two hydrothermal nontronites from weathered metamorphic rocks at the Uley graphite mine, South Australia. *Clays and Clay Minerals*, **48**, 537–548.

Khaled, E.M. and Stucki, J.W. (1991) Effects of iron oxidation state on cation fixation in smectites. *Soil Science Society of America Journal*, **55**, 550–554.

Kim, J.W., Dong, H., Seabaugh, J., Newell, S.W., and Eberl, D.D. (2004) Role of microbes in the smectite-to-illite reaction. *Science*, **303**, 830–832.

Komadel, P., Madejová, J., and Stucki, J. W. (2006) Structural Fe(III) reduction in smectites. *Applied Clay Science*, **34**, 88–94.

Kostka, J.E., Stucki, J.W., Nealson, K.H., and Wu, J. (1996) Reduction of structural Fe(III) in smectite by a pure culture of *Shewanella putrefaciens* strain MR-1. *Clays and Clay Minerals*, **44**, 522–529.

Kostka, J.E., Haefele, E., Viehweger, R., and Stucki, J.W. (1999) Respiration and dissolution of iron(III)-containing clay minerals by bacteria. *Environmental Science and Technology*, **33**, 3127–3133.

Kukkadapu, R.K., Zachara, J.M., Fredrickson, J.K., McKinley, J.P., Kennedy, D.W., Smith, S.C., and Dong, H. (2006) Reductive biotransformation of Fe in shale-limestone saprolite containing Fe(III) oxides and Fe(II)/Fe(III) phyllosilicates. *Geochimica et Cosmochimica Acta*, **70**, 3662–3676.

Lear, P.R. and Stucki, J.W. (1987) Intervalence electron transfer and magnetic exchange in reduced nontronite. *Clays and Clay Minerals*, **35**, 373–378.

Lear, P.R. and Stucki, J.W. (1989) Effects of iron oxidation state on the specific surface area of nontronite. *Clays and Clay Minerals*, **37**, 547–552.

Lee, K., Kostka, J.E., and Stucki, J.W. (2006) Comparisons of structural Fe reduction in smectites by bacteria and dithionite: An infrared spectroscopic study. *Clays and Clay Minerals*, **54**, 195–208.

Li, Y.-L., Vali, H., Sears, S.K., Yang, J., Deng, B., and Zhang, C.L. (2004) Iron reduction and alteration of nontronite NAu-2 by a sulfate-reducing bacterium. *Geochimica et Cosmochimica Acta*, **68**, 3251–3260.

Lieser, K.H. and Bauscher, C. (1988) Technetium in the hydrosphere and in the geosphere: influence of pH of complexing agents and of some minerals on the sorption of technetium. *Radiochimica Acta*, **44**, 125–128.

Liu, C., Zachara, J.M., Zhong, L., Kukkadupa, R., Szecsody, J.E., and Kennedy, D.W. (2005) Influence of sediment bioreduction and reoxidation on uranium sorption. *Environmental Science and Technology*, **39**, 4125–4133.

Lloyd, J.R., Sole, V.A., Van Praagh, C.V.G., and Lovley, D.R. (2000) Direct and Fe(II)-mediated reduction of technetium by Fe(III)-reducing bacteria. *Applied and Environmental Microbiology*, **66**, 3743–3749.

Luther, G.W., Shellenbarger, A., and Brendel, P.J. (1996) Dissolved organic Fe(III) and Fe(II) complexes in salt marsh porewaters. *Geochimica et Cosmochima Acta*, **60**, 951–960.

Manceau, A., Lanson, B., Drits, V.A., Chateigner, D., Gates, W.P., Wu, J., Huo, D., and Stucki, J.W. (2000a) Oxidation-reduction mechanism of iron in dioctahedral smectites. 1. Crystal chemistry of oxidized reference nontronites. *American Mineralogist*, **85**, 133–152.

Manceau, A., Lanson, B., Drits, V.A., Chateigner, D., Wu, J., Huo, D., Gates, W.P., and Stucki, J. W. (2000b) Oxidation-reduction mechanism of iron in dioctahedral smectites. 2. Structural chemistry of reduced Garfield nontronite. *American Mineralogist*, **85**, 153–172.

Morris, H.D., Shelton, B., and Ellis, P.D. (1990) ^{27}Al NMR spectroscopy of iron bearing montmorillonite clays. *Journal*

of Physical Chemistry, **94**, 3121–3129.
Morrison, S.R. (1980) *Electrochemistry at Semiconductor and Oxidized Metal Electrodes*. Plenum, New York.
NAGRA (2002) *Project Opalinus Clay: Safety report. Demonstration of disposal feasibility for spent fuel, vitrified high-level waste and long lived intermediate level waste*. NAGRA Technical Report NTB 02-05, Nagra, Wettingen, Switzerland.
O'Reilly, S.E., Watkins, J., and Furukawa, Y. (2005) Secondary mineral formation associated with respiration of nontronite, NAu-1 by iron reducing bacteria. *Geochemical Transactions*, **6**, 67–78.
O'Reilly, S.E., Furukawa, Y., and Newell, S. (2006) Dissolution and microbial Fe(III) reduction of nontronite (NAu-1). *Chemical Geology*, **235**, 1–11.
Qafoku, N.P., Ainsworth, C., Szecsody, J.E., Qafoku, O.S., and Heald, S.M. (2003) Effect of coupled dissolution and redox reactions on $Cr(VI)_{aq}$ attenuation during transport in the sediments under hyperalkaline conditions. *Environmental Science and Technology*, **37**, 3640–3646.
Rhoades, J.D., Ingvalson, R.D. and Stumpf, H.T. (1969) Interlayer spacing of expanded clay minerals at various swelling pressures: an X-ray diffraction technique for direct determination. *Soil Science Society of America Journal*, **33**, 473–475.
Riley, R.G. and Zachara, J.M. (1992) *Chemical Contaminants on DOE Lands and Selection of Contaminant Mixtures for Subsurface Science Research*. U.S. Department of Energy, Washington, D.C.
Rozenson, I. and Heller-Kallai, L. (1976) Reduction and oxidation of Fe(III) in dioctahedral smectite-l: reduction with hydrazine and dithionite. *Clays and Clay Minerals*, **24**, 271–282.
Scott, A.D. and Amonette, J. (1988) *The Role of Iron in Mica Weathering.* NATO ASI Series, C**:** pp. 537–623.
Shen, S. and Stucki, J.W. (1994) Effects of iron oxidation state on the fate and behavior of potassium in soils. Pp 173–185 in: *Soil Testing: Prospects for Improving Nutrient Recommendations* (J.L. Havlin, J. Jacobsen, P. Fixen, and G. Hergert, editors). SSSA Special Publication, **40**. Soil Science Society of America, Madison, Wisconsin.
Silvester, E., Charlet, L., Tournassat, C., Gehin, A., Greneche, J.-M., and Liger, E. (2005) Redox potential measurements and Mössbauer spectrometry of Fe(II) adsorbed onto Fe(III) (oxyhydr)oxides. *Geochimica et Cosmochimica Acta*, **69**, 4801–4815.
Skinner, M.F., Zabowski, D., Harrison, R., Lowe, A., and Xue, D. (2001) Measuring the cation exchange capacity of forest soils. *Communications in Soil Science and Plant Analysis*, **32**, 1751–1764.
Sposito, G. and Prost, R. (1982) Structure of water adsorbed on smectites. *Chemical Revisions*, **82**, 553–573.
Stookey, L.L. (1970) Ferrozine – a new spectrophotometric reagent for iron. *Analytical Chemistry*, **42**, 779–781.
Stucki, J.W. (2006) Iron redox processes in clay minerals. Pp. 429–482 in: *Handbook of Clay Science* (F. Bergaya, G. Lagaly, and B.K.G. Theng, editors). Elsevier, Amsterdam.
Stucki, J.W. and Huo, D. (1996) *Effects of Cation Competition on Potassium Fixation*. Proceedings of the Illinois Fertilizer Conference, Illinois.
Stucki, J.W. and Kostka, J.E. (2006) Microbial reduction of iron in smectite. *Comptes Rendus Geoscience*, **338**, 468–475
Stucki, J.W., Golden, D.C., and Roth, C.B. (1984a) Preparation and handling of dithionite-reduced smectite suspensions. *Clays and Clay Minerals*, **32**, 191–197.
Stucki, J.W., Golden, D.C., and Roth, C.B. (1984b) Effect of reduction and reoxidation of structural iron on the surface charge and dissolution of dioctahedral smectites. *Clays and Clay Minerals*, **32**, 350–356.
Stucki, J.W., Lee, K., Zhang, L., and Larson, R.A. (2002) The effects of iron oxidation state on the surface and structural properties of smectites. *Pure and Applied Chemistry*, **74**, 2079–2092.
Stumm, W. and Morgan, J.J. (1996) *Aquatic Chemistry.* Wiley, New York.
Taylor, R.W., Shen, S., Bleam, W.F., and Tu, S.I. (2000) Chromate removal by dithionite-reduced clays: evidence from direct X-ray absorption near edge spectroscopy (XANES) of chromate reduction at clay surfaces. *Clays and Clay Minerals*, **48**, 648–654.
Viani, B.E., Low, P.F., and Roth, C.B. (1983) Direct measurement of the relation between interlayer force and interlayer distance in the swelling of montmorillonite. *Colloidal and Interface Science*, **96**, 229–244.
Weissmahr, K.W., Haderlein, S.B., Schwarzenbach, R.P., Hany, R., and Nuesch, R. (1996) In situ spectroscopic investigations of adsorption mechanisms of nitroaromatic compounds at clay minerals. *Environmental Science and Technology*, **31**, 240–247.
Wildung, R.E., Gorby, Y.A., Krupka, K.M., Hess, N.J., Li, S.W., Plymale, A.E., McKinley, J.P., and Fredrickson, J.K. (2000) Effect of electron donor and solution chemistry on products of dissimilatory reduction of technetium by *Shewanella putrefaciens*. *Applied and Environmental Microbiology,*, 66, 2451–2460.
Wildung, R.E., Li, S.W., Murray, C.J., Krupka, K.M., Xie, Y., Hess, N.J., and Roden, E.E. (2004) Technetium reduction in sediments of a shallow aquifer exhibiting dissimilatory iron reduction potential. *FEMS Microbiology and Ecology*, **49**, 151–162.
Williams, A.G.B., and Scherer, M.M. (2004) Spectroscpoic evidence for Fe(II)-Fe(III) electron transfer at iron oxide-water interface. *Environmental Science and Technology*, **38**, 4782–4790.
Wu, J., Roth, C.B., and Low, P.F. (1988) Biological reduction of structural iron in sodium-nontronite. *Soil Science Society of America Journal*, **52**, 295–296.
Zachara, J.M., Fredrickson, J.K., Li, S.W., Kennedy, D.W., Smith, S.C., and Gassman, P.L. (1998) Bacterial reduction of crystalline Fe(III) oxides in single phase suspension and subsurface materials. *American Mineralogist*, **83**, 1426–1443.
Zachara, J.M., Heald, S.M., Jeon, B.-H., Kukkadapu, R.K., Dohnalkova, A.C., McKinley, J.P., Moore, D.A., and Liu, C. (2007) Reduction of pertechnetate [Tc(VII)] by aqueous Fe(II) and the nature of solid phase redox products. *Geochimica et Cosmochimica Acta*, **71**, 2137–2157.

(*Received 23 April 2007; revised 14 December 2007; Ms. 0023; A.E. H. Stanjek*)